Korean J. Chem. Eng., **30**(1), 145-153 (2013)
DOI: 10.1007/s11814-012-0101-5

Sorption and desorption kinetics of PAHs in coastal sediment

Sanghwa Oh*, Qiliang Wang, Won Sik Shin*,†, and Dong-Ik Song****

*Department of Environmental Engineering, Kyungpook National University, Daegu 702-701, Korea
**Department of Chemical Engineering, Kyungpook National University, Daegu 702-701, Korea
(*Received 23 March 2012 • accepted 23 June 2012*)

Abstract−Sorption and desorption kinetics of PAHs (naphthalene, phenanthrene and pyrene) in coastal sediment were investigated. Several kinetic models were used to analyze the kinetics: one-site mass transfer model (OSMTM), pseudo-first-order kinetic model (PFOKM), pseudo-second-order kinetic model (PSOKM), two compartment first-order kinetic model (TCFOKM) and modified two compartment first-order kinetic model (MTCFOKM). Among the models, the MTCFOKM was the best in fitting both sorption and desorption kinetic data, and therefore could predict the most accurately. In MTCFOKM, the fast sorption fraction ($f'_{1,s}$) increased with the hydrophobicity (K_{ow}) of the PAHs, whereas the fast desorption fraction ($f'_{1,d}$) decreased. The fast sorption rate constant ($k'_{1,s}$) was much greater than the slow sorption rate constant ($k'_{2,s}$). Effect of aging on the desorption kinetics was also analyzed. The $f'_{1,d}$ in MTCFOKM decreased but the slow desorption fraction ($f'_{2,d}$) increased with aging, indicating that slow desorption is directly related to aging.

Key words: Sorption, Desorption, Model, Kinetics, Sediment

INTRODUCTION

Sediments act as sinks for many organic compounds [1]. Polycyclic aromatic hydrocarbons (PAHs) have been also acknowledged as one of the most representative of them. Many PAHs are easily sorbed onto suspended particles or sediments due to their high hydrophobicity [2,3]. Sorption and desorption of hydrophobic organic compounds (HOCs) in sediments is an underlying process affecting the transport and degradation of organic compounds in the environment. Numerous studies have shown that an understanding of the dynamics of sorption and desorption is crucial to the transport and risk assessment models, which contain terms for sorption and desorption, but the mechanisms governing sorption and desorption rates are not fully understood [4-7].

Many studies have investigated sorption and desorption kinetics of HOCs in sediments and used such data to infer possible mechanisms [8-10]. The major factors controlling sorption and desorption include the hydrophobicity of the solute and the organic carbon content, mineral composition, and surface area of the sorbents [10-12]. A complete description of sorption and desorption in sediments should take into account numerous phenomena, including solution phase reactions, surface reactions, and mass transport phenomena [13]. The intraorganic matter diffusion was responsible for the sorption nonequilibrium of HOCs and intraorganic matter diffusion plus chemical nonequilibrium for polar organic chemicals [14]. The occurrence of biphasic rates of sorption or desorption in sediments and soils, involving a fast initial uptake followed by a slow stage to apparent equilibrium have been widely accepted [11,15].

However, there is not available information on the effect of salinity on the sorption/desorption kinetics of PAHs in sediments under freshwater, estuarial and coastal conditions featuring temporal and spatial gradients of salinity [16]. Yang and Zheng [3] reported that PAHs sorption is very rapid, but equilibration time was slightly longer in deionized water than in natural seawater. Koelmans et al. [14] also reported that fast desorption in fresh sediment was interpreted as molecular diffusion and slow desorption was consistent with log K_{ow} and intraorganic matter diffusion. However, there is not available report on the desorption kinetics of PAHs in coastal sediment.

In this work, sorption and desorption kinetic experiments of three PAHs (naphthalene, phenanthrene and pyrene) in a coastal sediment were carried out in a batch-type adsorber and were analyzed using the one-site mass transfer model (OSMTM), the pseudo-first-order kinetic model (PFOKM), the pseudo-second-order kinetic model (PSOKM), the two compartment first-order kinetic model (TCFOKM) and the modified two compartment first-order kinetic model (MTCFOKM). The objective of this study is to examine sorption and desorption kinetics of PAHs in natural coastal sediment. The results of this study will provide a valuable insight into developing remediation strategies for coastal sediment polluted with PAHs.

MATERIALS AND METHODS

1. Sediment

The sediment sample was collected from the surface layer (0-20 cm) of coastal sediment in Suncheon, Jeollanam-do, Korea. The sediment was air-dried, sieved through a U.S. Sieve Series No. 20 sieve to remove debris, shell and live organisms. The sediment was then washed with deionized water to remove interstitial and readily desorbing colloidal solids that may alter partitioning constants of neutral hydrophobic compounds. After washing, the sediment was air-dried, homogenized, placed in an amber bottle and stored in the refrigerator prior to use. The sediment properties analyzed by Huffmann Laboratories, Inc. (Golden, CO, USA) are summarized in Table 1. Brunauer-Emmett-Teller (BET) surface area was determined by specific surface area analyzer (Micromeritics, ASAP-2010).

†To whom correspondence should be addressed.
E-mail: wshin@mail.knu.ac.kr

Table 1. Summary of sediment characteristics analyzed by Huffman Laboratory (Golden, Co, USA). Data indicate percentages (%) based on dry weight

Total carbon (wt%)	0.28
Carbonate carbon (wt%)	0.03
Organic carbon (wt%)	0.25
Nitrogen (wt%)	0.03
BET-surface area (m^2/g)	4.2

A preliminary study on the sediment analysis using a gas chromatography/mass spectrometry (GC/MS) showed that the sediment was not contaminated with PAHs (data not shown).

2. Chemicals

Radiolabeled [1-^{14}C] naphthalene (ChemSyn Labortories, Inc., 58.4 mCi/mmol, >98%), [9-^{14}C] phenanthrene (ARC, 55 mCi/mmol, >98%) and [4,5,9,10-^{14}C] pyrene (ChemSyn Laboratories, Inc., 53.2 mCi/mmol, >98%) were used as radiotracer. ^{12}C-naphthalene (>99 +%, Aldrich), phenanthrene (>96%, Sigma) and pyrene (>96%, Aldrich) were used as received. The ^{14}C-PAHs were further diluted with unlabeled ^{12}C-PAHs stock solutions (1,000 mg/L in methanol) to yield desired concentrations. The physicochemical properties of PAHs were listed in Table 2. Sodium azide (200 mg/L) was added to the solution as a bacterial inhibitor. The PAH solutions were prepared before sorption experiment using the ^{14}C stock solutions and the artificial seawater (pH=7.5). The salinity was controlled at 30‰. The chemical composition of the artificial seawater was 24.72 g/L of NaCl, 0.67 g/L of KCl, 1.36 g/L of $CaCl_2 \cdot 2H_2O$, 2.18 g/L of $MgCl_2$, 3.07 g/L of $MgSO_4$, 0.18 g/L of $NaHCO_3$ and 0.20 g/L of NaN_3 [18, 19].

3. Sorption Kinetics

Sorption kinetic studies were conducted in batch mode using 40-mL amber glass vials (Fisher Co.) with Teflon-faced silicone septa. Control experiments without sediment were conducted to investigate loss of PAHs due to sorption onto the surface of the glassware (data not shown). The concentrations of PAHs remained essentially unchanged.

The vials containing sediment (5.0 g for naphthalene and 2.0 g of sediment for phenanthrene and pyrene, respectively) were carefully filled with the PAH stock solutions minimizing the head space. The initial concentrations of the PAHs were 20 mg/L for naphthalene, 0.7 mg/L for phenanthrene and 0.07 mg/L for pyrene, respectively, and the initial radioactivity was approximately 2,000 cpm/mL. The vials were placed on an orbital shaker and then shaken at 20 °C and 150 rpm.

After predetermined time intervals (1 hr to 16 d), the vials were collected and centrifuged for 20 min at 2,500 rpm. The chemical concentration in the supernatant was analyzed by liquid scintillation counting. 1 mL of the supernatant was mixed with 8 mL of scintillation cocktail (Ultima Gold, Sigma-Aldrich) and the radioactivity was determined by liquid scintillation counter (LSC, EG&G Wallac Co., 1220 Quantulus). The solid phase equilibrium concentrations were calculated by assuming all concentration changes in solution phase result from sorption onto the solid phase. All experiments were run in duplicate.

4. Effect of Aging on Desorption Kinetics

To investigate the effect of aging (or contact time) on desorption kinetics, desorption experiments were conducted using the solute-loaded sediments obtained from the preceding sorption experiments (i.e., sorption equilibration time=2 d, 30 d and 100 d). The 40 mL amber vials containing sediments (5.0 g for naphthalene, 2.0 g for phenanthrene and 1.0 g for pyrene, respectively) were filled with the PAH stock solutions minimizing headspace. The initial concentrations of the PAHs were 20 mg/L for naphthalene, 0.7 mg/L for phenanthrene and 0.07 mg/L for pyrene, respectively, and the initial radioactivity was approximately 2,000 cpm/mL. The vials were placed on an orbital shaker and shaken for 2 d, 30 d, and 100 d, respectively, at 20 °C and 150 rpm prior to desorption experiments.

After aging, the vials were collected and centrifuged for 20 minutes at 2,500 rpm. After centrifugation, 1 mL of the supernatant was mixed with 8 mL of scintillation cocktail (Ultima Gold, Sigma) and the radioactivity was analyzed via liquid scintillation counting. Approximately 95% of the supernatant was carefully removed using a pipette and replaced with solute-free artificial seawater (30‰). The exact amount of the supernatant removed was determined gravimetrically, and non-zero initial concentration of the aqueous solution in the desorption stage was computed from the mass balance accordingly. The vials were vortexed for 20 seconds, placed on an orbital shaker

Table 2. Physicochemical properties of PAHs used

	Naphthalene	Phenanthrene	Pyrene
MW (g/mol)	128.17	178.23	202.26
Solubility (mg/L) at 0‰[a]	31	1.15	0.135
Solubility (mg/L) at 30‰	23.9[b]	0.742[b]	0.0914[b]
log K_{ow}	3.30	4.46	4.88
Melting point (°C)	80.6	99	156
Boiling point (°C)	218	340	404
Molecular structure	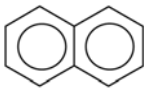	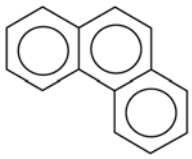	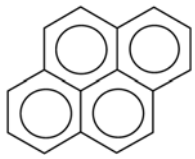

[a]‰: Part per thousand

[b]Calculated by using Setschenow equation [17]

at 20 °C and shaken at 150 rpm. After predetermined time intervals (1 hr to 16 d), the sorbent was separated from the solution by centrifuging for 30 minutes at 2,500 rpm. The aqueous phase equilibrium concentration was determined by liquid scintillation counting. The concentrations of PAHs remaining in the solid phase were calculated by assuming all concentration changes in solution phase result from desorption from the solid phase. All experiments were run in duplicate.

SORPTION AND DESORPTION KINETIC MODELS

1. One-site Mass Transfer Model (OSMTM)

One-site mass transfer model (OSMTM) for sorption rate was proposed by Nzengung et al. [20]. In OSMTM, sorption rate was represented as a first-order function of the concentration difference between the solution and sorbed phases under the assumption of the linear sorption equilibrium. The proposed equations for sorption and desorption were Eqs. (1) and (2), respectively [20-22].

$$\frac{C(t)}{C_0}=\frac{C_e}{C_0}+\left(1-\frac{C_e}{C_0}\right)\exp\left[\left(-\frac{C_0}{C_e}k_s\right)t\right] \tag{1}$$

where C(t) denote the solute concentrations in the solution (mg/L) phase at time t (day) and k_s is the mass transfer coefficient (1/day) for sorption between the solution and solid phase. C_0 and C_e denote initial and equilibrium concentrations in the solution phase respectively.

$$\frac{q(t)}{q_0}=\frac{q_e}{q_0}+\left(1-\frac{q_e}{q_0}\right)\exp\left[\left(-\frac{q_0}{q_e}k_d'\right)t\right] \text{ where } k_d'\equiv k_d K_{p,d}\left(\frac{C_0}{q_0}+\frac{W}{V}\right) \tag{2}$$

where q(t) denotes the solute concentration in the solid phase (mg/kg) at time t (day) and q_0 and q_e are initial and equilibrium concentrations in solid phase (mg/kg), respectively. k_d and $K_{p,d}$ are the mass transfer coefficient (1/day) and partition coefficient (L/kg) for desorption, respectively. V and W are the volume of the solution phase (L) and the sorbent weight (g), respectively. Furthermore, the desorption mass transfer coefficient, k_d should be determined from the apparent mass transfer coefficient for desorption (k_d', 1/day) to compare with the sorption mass transfer coefficient, k_s.

2. Pseudo-first-order Kinetic Model (PFOKM)

The Lagergren pseudo-first-order model has been widely used to predict sorption kinetics, Eq. (3) [23]. For sorption, Eq. (4) was used:

$$\frac{dC(t)}{dt}=-k_{p1,s}C(t) \tag{3}$$

$$\frac{C(t)}{C_0}=1-\frac{q_{e,s}}{C_0}\cdot\frac{W}{V}(1-e^{-k_{p1,s}t}) \tag{4}$$

where $k_{p1,s}$ is the rate constant of pseudo-first-order sorption (1/day) and $q_{e,s}$ is the sorption equilibrium concentration in the solid phase (mg/kg), respectively.

Similarly, the pseudo-first-order equation for desorption can be derived as:

$$\frac{q(t)}{q_0}=\frac{q_{e,d}}{q_0}+\left(1-\frac{q_{e,d}}{q_0}\right)e^{-k_{p1,d}t} \tag{5}$$

where $k_{p1,d}$ is the rate constant of pseudo-first-order desorption (1/day) and $q_{e,d}$ is the sorption equilibrium concentration in the solid phase (mg/kg), respectively.

3. Pseudo-second-order Kinetic Model (PSOKM)

The pseudo-second-order equation based on sorption equilibrium capacity is expressed as [23,24]:

$$\frac{C(t)}{C_0}=1-\frac{1}{C_0}\cdot\frac{(W/V)\cdot t}{1/(k_{p2,s}q_{e,s}^2)+t/q_{e,s}} \tag{6}$$

where $k_{p2,s}$ is the rate constant of pseudo-second-order sorption (kg/mg/day).

Similarly, the pseudo-second-order equation for desorption can be derived as [25]:

$$\frac{q(t)}{q_0}=\frac{1+k_{p2,d}\left(q_{e,d}-\frac{q_{e,d}^2}{q_0}\right)t}{1+k_{p2,d}(q_0-q_{e,d})t} \tag{7}$$

where $k_{p2,d}$ is the rate constant of pseudo-second-order desorption (kg/mg/day).

The constant $k_{p2,s}$ or $k_{p2,d}$ is used to calculate the initial sorption ($v_{0,s}$, mg/kg/day) or desorption rate ($v_{0,d}$, mg/kg/day) at $t\rightarrow 0$, as follows [25]:

$$v_{o,s}=k_{p2,s}q_{e,s}^2 \text{ or } v_{o,d}=k_{p2,d}(q_0-q_{e,d})^2 \tag{8}$$

4. Two Compartment First-order Kinetic Model (TCFOKM)

The overall sorption (or desorption) in the two compartment first-order kinetic model (TCFOKM) was assumed to consist of the sum of the two first-order sorption (or desorption) rates in the fast and slow fractions [21,22,25-28]:

$$\frac{C(t)}{C_0}\left(\text{or } \frac{q(t)}{q_0}\right)=f_1e^{-k_1t}+(1-f_1)e^{-k_2t} \tag{9}$$

where f_1 and f_2 (=1−f_1) are the fast and slow sorption (or desorption) fractions (−), respectively, and k_1 and k_2 are the sorption (or desorption) rate constants in the fast and slow fractions (day^{-1}), respectively. However, the TCFOKM is mathematically wrong because both exponential terms in the right-hand side of Eq. (9) becomes 0 as $t\rightarrow\infty$ (i.e., $e^{-\infty}=0$) and thus left-hand side term also becomes 0 (i.e., $C(t)/C_0$ or $q(t)/q_0\rightarrow 0$).

5. Modified Two Compartment First-order Kinetic Model (MTCFOKM)

To overcome the mathematical limitations of the TCFOKM, we propose a modified TCFOKM (MTCFOKM) for sorption [22]:

$$\frac{q_e-q(t)}{q_e-q_0}=f_{1,s}'e^{-k_{1,s}'t}+(1-f_{1,s}')e^{-k_{2,s}'t} \tag{10}$$

where $f_{1,s}'$ and $f_{2,s}'$ are the fast and slow sorption fractions (−), respectively, and $k_{1,s}'$ and $k_{2,s}'$ are the sorption rate constants in the fast and slow fractions (day^{-1}), respectively. In Eq. (10), $q(t)\rightarrow q_0$ as $t\rightarrow 0$ and $q(t)\rightarrow q_e$ as $t\rightarrow\infty$.

Using the mass balance, $W(q-q_0)=V(C_0-C)$, following equations are obtained:

$$\frac{C(t)-C_e}{C_0-C_e}=f_{1,s}'e^{-k_{1,s}'t}+(1-f_{1,s}')e^{-k_{2,s}'t} \tag{11}$$

$$\text{or } \frac{C(t)}{C_0}=\frac{C_e}{C_0}+\left(1-\frac{C_e}{C_0}\right)[f_{1,s}'e^{-k_{1,s}'t}+(1-f_{1,s}')e^{-k_{2,s}'t}] \tag{12}$$

In Eqs. (10) and (11), $C(t) \rightarrow C_0$ as $t \rightarrow 0$ and $C(t) \rightarrow C_e$ as $t \rightarrow \infty$. MTCFOKM, Eq. (10) or Eq. (11) is similar to TCFOKM, Eq. (9), but it includes q_e or C_e in the numerator and denominator of the left-hand side of the equations. Eq. (12) is also similar to the OSMTM, Eq. (1). The difference is that OSMTM has one exponential term but MTCFOKM has two.

Similarly, a MTCFOKM for desorption can be derived using the mass balance, $W(q-q_0)=V(C_0-C)$ [22]:

$$\frac{q(t)}{q_0} = \frac{q_e}{q_0} + \left(1-\frac{q_e}{q_0}\right)[f'_{1,d}e^{-k'_{1,d}t} + (1-f'_{1,d})e^{-k'_{2,d}t}] \quad (13)$$

where $f'_{1,d}$ and $f'_{2,d}$ are the fast and slow sorption fractions, respectively, and $k'_{1,d}$ and $k'_{2,d}$ are the desorption rate constants in the fast and slow fractions (day^{-1}), respectively. In Eq. (13), $q(t) \rightarrow q_0$ as $t \rightarrow 0$ and $q(t) \rightarrow q_e$ as $t \rightarrow \infty$. Eq. (13) is also similar to the OSMTM, Eq. (2).

All model parameters were estimated by non-linear regression using a commercial software package, TableCurve 2D® (Version 5.1, SYSTAT Software, Inc.).

RESULTS AND DISCUSSION

1. Sorption Kinetics

Sorption of naphthalene, phenanthrene and pyrene over time onto the coastal sediment is shown in Fig. 1. The sorption kinetic models were fitted to the sorption kinetic data and the fitted model parameters are summarized in Tables 3 to 7.

As indicated by the R^2 values in Tables 3 to 7, the three-parameter TCFOKM ($R^2>0.95$) and 4-parameter MTCFOKM ($R^2>0.98$) fitted better than the two-parameter OSMTM ($R^2>0.85$), PFOKM ($R^2>0.85$), and PSOKM ($R^2>0.90$) as expected from the number of parameters involved in the models.

As can be seen from Table 3 (OSMTM), apparent sorption equilibria (C_e) were observed within 1 day. In other words, a substantial portion of the solute was sorbed within 1 day, followed by a slow sorption over 16 days of sorption period. The mass transfer coefficient for sorption (k_s) was inversely related to the hydrophobicity (log K_{ow}).

The pseudo-first-order kinetic model (PFOKM) was also used to analyze sorption kinetics. In Table 4, the sorption rate constant of PFOKM ($k_{p1,s}$) increased in the order of pyrene (154.5 day^{-1})> naphthalene (41.4 day^{-1})≥phenanthrene (40.7 day^{-1}) that is not same as the order of increase in hydrophobicity (pyrene>phenanthrene >naphthalene). Comparison of R^2 values (Tables 3 and 4) showed that PFOKM had nearly the same goodness of fit as OSMTM.

The pseudo-second-order kinetic model (PSOKM) was also used to analyze sorption kinetics. As listed in Table 5, the sorption rate constant of PSOM ($k_{p2,s}$) was in the order of pyrene (746.8 kg/mg/day)>phenanthrene (9.594 kg/mg/day)>naphthalene (1.455 kg/mg/day), corresponding to the log K_{ow}. The more hydrophobic PAH had the higher $k_{p2,s}$. However, the initial sorption rate ($v_{0,s}$) was in the order of naphthalene (3,850 mg/kg/day)>pyrene (1,447 mg/kg/day)>phenanthrene (628.5 mg/kg/day), different from the order of log K_{ow} because C_0 and $q_{e,s}$ values were not same for each PAH. Comparison of R^2 values (Tables 3 to 5) showed that PSOKM fitted better than OSMTM and PFOKM to the sorption kinetic data.

The results of TCFOKM analysis for sorption (Table 6) showed

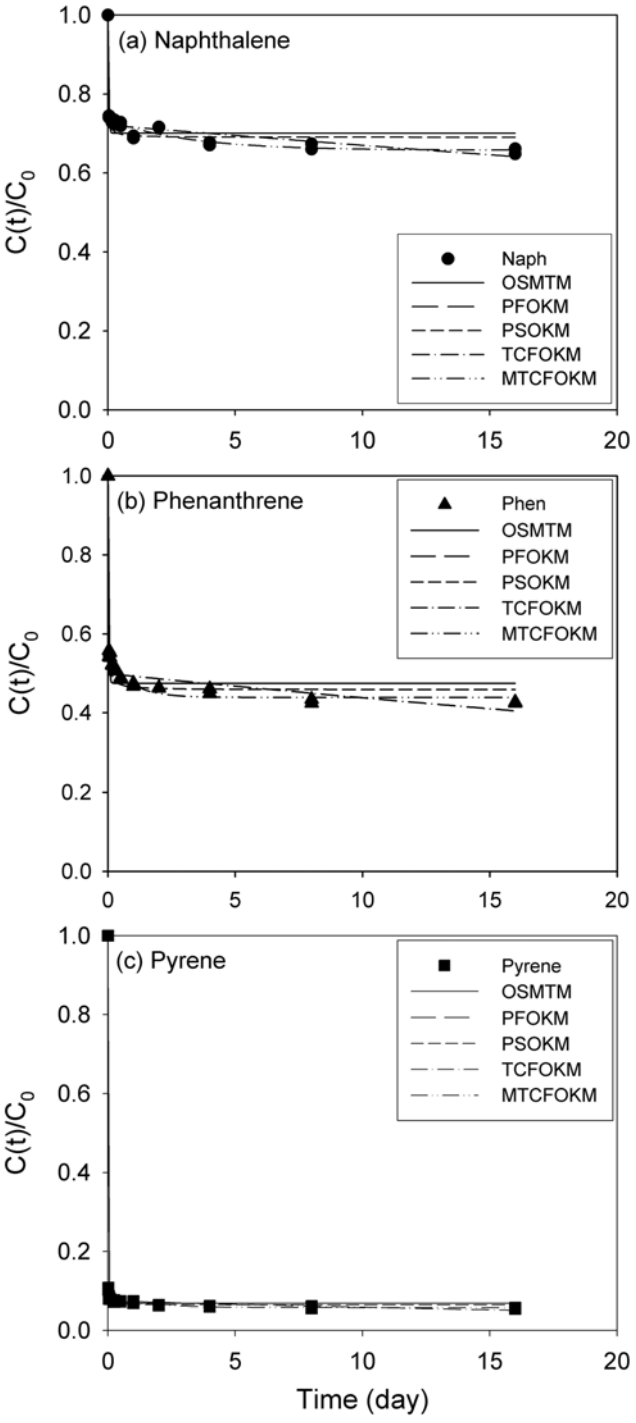

Fig. 1. Sorption kinetics of PAHs onto coastal sediment: (a) naphthalene, (b) phenanthrene and (c) pyrene.

that the fast sorption fraction (f_1) increased, while the slow sorption fraction (f_2) decreased as the hydrophobicity (log K_{ow}) of the PAHs increased and both $k_{1,s}$ and $k_{1,s}$ also increased with log K_{ow}. For all PAHs, the sorption rate constant of fast sorption fraction ($k_{1,s}$) was much greater than that of slow sorption fraction ($k_{2,s}$). Comparison of R^2 values (Tables 2 to 6) shows that the three-parameter TCFOKM fitted the sorption data better than the two-parameter OSMTM and PSOKM as expected from the number of fitting parameters involved in each model (i.e., three *vs.* two). The first-order sorption rate con-

Table 3. One-site mass transfer model (OSMTM) parameters for sorption and desorption kinetics of PAHs in sediment. t_{eq}=equilibration time (day)

Process	Solute		C_0 (mg/L)	C_e (mg/L)	k_s (day^{-1})		t_{eq} (day)	R^2	SSE
Sorption	Naph		20	14.02±0.140	29.03±6.59		0.17	0.8453	0.0156
	Phen		0.7	0.332±0.006	19.35±3.10		0.25	0.9525	0.0246
	Pyr		0.07	0.005±0.0001	10.65±0.74		0.08	0.9990	0.0015
Desorption	Solute	Aging (day)	q_0 (mg/kg)	q_e (mg/kg)	k_d' (day^{-1})	k_d (day^{-1})	t_{eq} (day)	R^2	SSE
	Naph	2	43.10	31.01±0.340	21.12±3.346	10.67±1.691	0.50	0.8921	0.0180
		30	50.39	39.51±0.313	33.09±5.979	12.18±2.201	0.25	0.8790	0.0117
		100	57.56	48.08±0.302	42.91±9.327	11.97±2.601	0.25	0.8497	0.0081
	Phen	2	8.69	6.90±0.051	9.58±1.429	2.707±0.404	1.0	0.8586	0.0087
		30	9.20	7.02±0.070	6.36±1.224	2.104±0.405	1.0	0.7788	0.0143
		100	9.30	7.15±0.070	9.10±2.079	2.910±0.665	1.0	0.6893	0.0157
	Pyr	2	1.38	1.29±0.001	60.77±8.018	4.344±0.573	0.08	0.9511	0.0004
		30	1.41	1.34±0.007	75.97±9.890	4.067±0.529	0.08	0.9641	0.0002
		100	1.42	1.37±0.001	91.25±16.91	3.179±0.589	0.04	0.9481	0.0001

Table 4. Pseudo-first-order kinetic model (PFOKM) parameters for sorption and desotion kinetics of PAHs in sediment

Process	Solute		C_0 (mg/L)	$q_{e,s}$ (mg/kg)	$k_{p1,s}$ (day^{-1})	R^2	SSE
Sorption	Naph		20	0.0494±0.0012	41.42±9.237	0.8453	0.0156
	Phen		0.7	0.0078±0.0001	40.74±6.228	0.9525	0.0246
	Pyr		0.07	0.0014±0.0000	154.5±8.288	0.9990	0.0015
	Solute	Aging (day)	q_0 (mg/kg)	$q_{e,d}$ (mg/kg)	$k_{p1,d}$ (day^{-1})	R^2	SSE
Desorption	Naph	2	43.10	31.01±0.340	29.36±4.518	0.8921	0.0180
		30	50.39	39.51±0.313	42.20±7.488	0.8790	0.0117
		100	57.56	48.08±0.302	51.36±11.04	0.8497	0.0086
	Phen	2	8.69	6.900±0.052	12.01±1.746	0.8595	0.0087
		30	9.20	7.441±0.074	7.917±1.486	0.7788	0.0143
		100	9.30	7.653±0.075	10.918±2.435	0.6893	0.0157
	Pyr	2	1.38	1.289±0.001	64.92±8.538	0.9511	0.0004
		30	1.41	1.336±0.001	79.94±10.39	0.9641	0.0002
		100	1.42	1.374±0.001	94.28±17.45	0.9481	0.0001

Table 5. Pseudo-second-order kinetic model (PSOKM) parameters for sorption and desorption kinetics of PAHs in sediment

Process	Solute		C_0 (mg/L)	$q_{e,s}$ (mg/kg)	$k_{p2,s}$ (kg/mg/day)	$v_{0,s}$ (mg/kg/day)	R^2	SSE
Sorption	Naph		20	51.44±1.455	1.455±0.5457	3,850	0.9693	0.0047
	Phen		0.7	8.094±0.131	9.594±1.731	628.5	0.9898	0.0047
	Pyr		0.07	1.392±0.002	746.8±77.19	1,447	0.9996	0.0006
	Solute	Aging (d)	q_0 (mg/kg)	$q_{e,d}$ (mg/kg)	$k_{p2,d}$ (kg/mg/day)	$v_{0,d}$ (mg/kg/day)	R^2	SSE
Desorption	Naph	2	43.10	30.55±0.237	3.718±0.557	585.4	0.9569	0.0072
		30	50.39	39.09±0.247	5.887±1.154	751.6	0.9328	0.0060
		100	57.56	47.76±0.276	9.045±2.588	868.0	0.8968	0.0059
	Phen	2	8.685	6.805±0.035	10.11±1.312	35.9	0.9517	0.0030
		30	9.199	6.914±0.055	6.435±1.229	33.6	0.8988	0.0065
		100	9.302	7.051±0.057	10.05±2.379	50.8	0.8450	0.0078
	Pyr	2	1.377	1.286±0.001	1,403±209.09	12.4	0.9783	0.0002
		30	1.406	1.335±0.001	2,548±408.32	14.3	0.9833	0.0001
		100	1.420	1.373±0.001	4,868±1369	10.8	0.9626	0.0001

Table 6. Two compartment first-order kinetic model (TCFOKM) parameters for sorption and desorption kinetics of PAHs in sediment

				Fast fraction		Slow fraction			
Process	Solute		C_0 (mg/L)	$f_{1,s}$	$k_{1,s}$ (day^{-1})	$f_{2,s}=1-f_{1,d}$	$k_{2,s}$ (day^{-1})	R^2	SSE
Sorption	Naph		20	0.279±0.005	57.46±11.92	0.721	0.0073±0.0012	0.9511	0.0049
	Phen		0.7	0.501±0.007	50.21±6.736	0.499	0.0131±0.0025	0.9808	0.0099
	Pyr		0.07	0.925±0.002	162.92±6.242	0.075	0.0241±0.0044	0.9997	0.0005
	Solute	Aging (d)	q_0 (mg/kg)	$f_{1,d}$	$k_{1,d}$ (day^{-1})	$f_{2,d}=1-f_{1,d}$	$k_{2,d}$ (day^{-1})	R^2	SSE
Desorption	Naph	2	43.10	0.263±0.009	36.02±5.656	0.737	0.0052±0.0019	0.9226	0.0129
		30	50.39	0.200±0.006	54.63±9.400	0.800	0.0046±0.0012	0.9309	0.0067
		100	57.56	0.151±0.005	71.87±15.40	0.849	0.0039±0.0009	0.9251	0.0043
	Phen	2	8.69	0.186±0.005	16.58±2.007	0.814	0.0048±0.0009	0.9411	0.0036
		30	9.20	0.160±0.006	14.13±2.271	0.840	0.0068±0.0011	0.9236	0.0049
		100	9.30	0.150±0.007	22.57±5.649	0.850	0.0056±0.0014	0.8275	0.0087
	Pyr	2	1.38	0.062±0.001	73.94±9.317	0.938	0.0006±0.0002	0.9692	0.0002
		30	1.41	0.049±0.001	88.50±11.94	0.952	0.0003±0.0001	0.9728	0.0001
		100	1.42	0.031±0.000	114.45±19.42	0.969	0.0004±0.0001	0.9780	0.00004

Table 7. Modified two compartment first-order kinetic model (MTCFOKM) parameters for sorption and desorption kinetics of PAHs sediment. Numbers in parenthesis indicate the standard deviation

					Fast fraction		Slow fraction			
Process	Solute		C_0 (mg/L)	$C_{e,s}$ (mg/L)	$f'_{1,s}$	$k'_{1,s}$ (day^{-1})	$f'_{2,s}$	$k'_{2,s}$ (day^{-1})	R^2	SSE
Sorption	Naph		20	13.20±0.193	0.777±0.028	90.44±55.32	0.223	0.405±0.179	0.9926	0.0011
	Phen		0.7	0.307±0.004	0.813±0.017	75.61±15.27	0.187	1.213±0.308	0.9985	0.0007
	Pyr		0.07	0.004±0.000	0.976±0.002	173.13±4.45	0.024	0.592±0.131	0.9999	0.0001
	Solute	Aging (d)	q_0 (mg/kg)	$q_{e,d}$ (mg/kg)	$f'_{1,d}$	$k'_{1,d}$ (day^{-1})	$f'_{2,d}$	$k'_{2,d}$ (day^{-1})	R^2	SSE
Desorption	Naph	2	43.10	30.21±0.121	0.174±0.007	160.09±63.12	0.826	2.975±0.397	0.9927	0.0012
		30	50.38	38.30±0.062	0.162±0.002	117.12±9.401	0.838	1.181±0.086	0.9983	0.0002
		100	57.56	46.86±0.337	0.134±0.007	129.47±57.57	0.866	0.678±0.299	0.9513	0.0028
	Phen	2	8.69	6.690±0.042	0.160±0.006	25.09±3.167	0.840	0.549±0.154	0.9758	0.0015
		30	9.20	7.120±0.038	0.127±0.004	26.84±3.258	0.873	0.427±0.066	0.9861	0.0009
		100	9.30	7.407±0.028	0.109±0.004	94.17±66.42	0.891	0.819±0.114	0.9846	0.0008
	Pyr	2	1.38	1.283±0.001	0.055±0.001	114.19±12.17	0.945	1.576±0.308	0.9957	0.0000
		30	1.41	1.333±0.001	0.043±0.001	154.65±31.64	0.957	2.167±0.580	0.9944	0.0000
		100	1.42	1.371±0.001	0.029±0.001	166.26±58.55	0.971	1.012±0.423	0.9856	0.0000

stants in the fast ($k_{1,s}$) and slow ($k_{2,s}$) fractions were found to 10^1-10^2 day^{-1} and 10^{-2}-10^{-3} day^{-1}, respectively. The precision of estimated $k_{2,s}$ is only good when experiments were conducted to near the time of $1/k_{2,s}$ (approximately 100 days). An extension of time frame to 100 days would be unrealistic for the sorption of PAHs in sorbents used in this study because most of the fast sorption fraction is sorbed within a few hours. Therefore, the precision of $k_{2,s}$ values obtained in this study may be unsatisfactory, and only an order of magnitude estimate is useful in interpreting the time frame for the sorption in the slow fraction. However, precision of $k_{1,s}$ in this study would be useful since the time frame in the fast fraction is 10^{-1}-10^{-2} day (i.e., $1/k_{1,s}$).

The results of MTCFOKM analysis for sorption kinetics (Table 7) showed that $f'_{1,s}$ and $k'_{1,s}$ were in the order of pyrene>phenanthrene>naphthalene corresponding to the hydrophobicity (log K_{ow}) of the PAHs; however, $k'_{2,s}$ was irregularly varied. This indicates that the fast sorption fraction and the rate are affected by hydrophobicity, but the slow sorption rate is not. For all PAHs, the sorption rate constant of fast sorption fraction ($k'_{1,s}$) was much greater than that of slow sorption fraction ($k'_{2,s}$). Comparison of R^2 values (Tables 2 to 5) showed that four-parameter MTCFOKM fitted the data better than the two-parameter OSMTM and PSOKM and the three-parameter TCFOKM as expected from the number of fitting parameters involved in each model. The first-order sorption rate constants in the fast ($k'_{1,s}$) and slow ($k'_{2,s}$) fractions were found to 10^1-10^2 day^{-1} and 10^{-1}-10^0 day^{-1}, respectively.

2. Desorption Kinetics

The desorption kinetic data of PAHs after aging are presented in Fig. 2. The desorption kinetic models were fitted to the desorption kinetic data and the model parameters were summarized in Tables 3 to 7.

In Table 3, the results of OSMTM analysis indicate that appar-

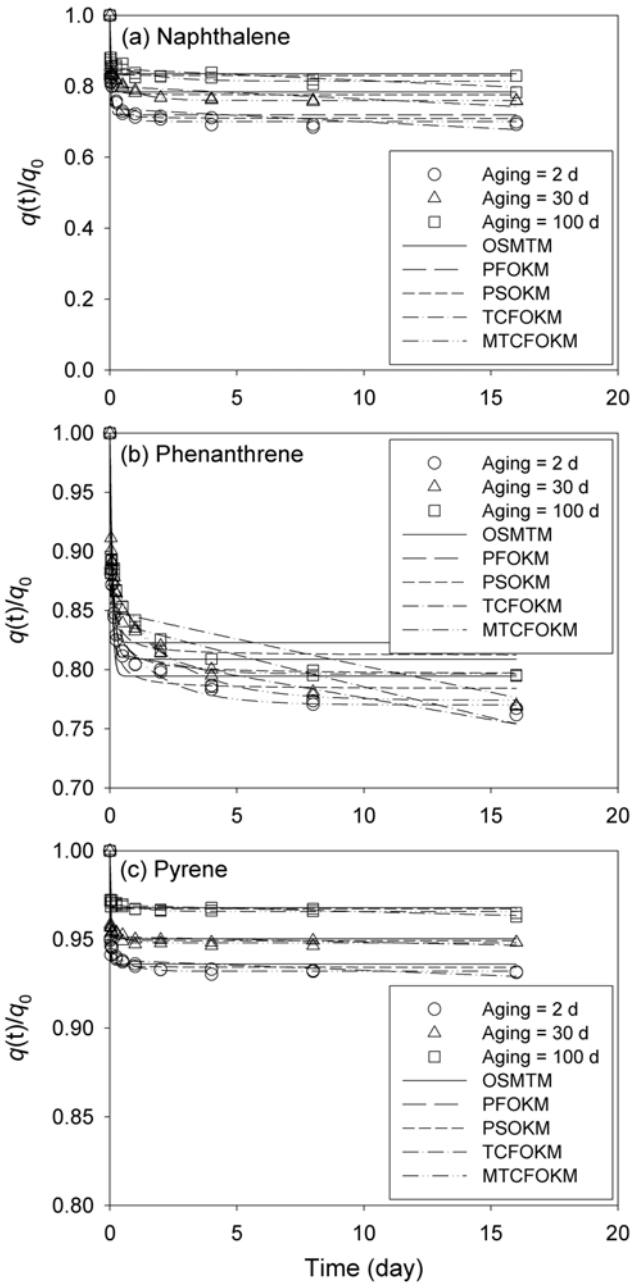

Fig. 2. Effect of aging time (2, 30 and 100 d) on the desorption kinetics of PAHs from coastal sediment: (a) naphthalene, (b) phenanthrene and (c) pyrene.

ent desorption equilibria were observed within the first 1 day. A substantial portion of the solute was desorbed within 1 d, followed by a slow desorption over 16 d of desorption period. The mass transfer coefficient for desorption (k_d) was not related to aging time. However, the apparent mass transfer coefficient for desorption (k_d') increased over contact time except phenanthrene (Table 3). Both k_d and k_d' were not correlated to the K_{ow} values of the PAHs.

As shown in Table 4, the desorption rate constant of PFOKM ($k_{p1,d}$) increased over aging time except phenanthrene. Comparison of PFOKM analysis for sorption and desorption kinetics shows that $k_{p1,d}$ is greater than $k_{p1,s}$ except naphthalene.

As shown in Table 5, the desorption rate constant of PSOKM ($k_{p2,d}$) increased over aging time except phenanthrene. Table 5 shows an increase in $v_{0,d}$ with hydrophobicity; however, it was caused by different initial concentrations of PAHs, not by hydrophobicity, and also shows poor relationship between $v_{0,d}$ and aging time. Comparison of PSOKM analysis for sorption and desorption kinetics (Table 5) showed that $k_{p2,d}$ was greater than $k_{p2,s}$ except phenanthrene at 100 d of aging time. Comparison of R^2 values (Tables 3 to 5) showed that the PSOKM was better fitted than OSMTM and PFOKM to desorption kinetic data. Overall, all the two-parameter kinetic models were not able to describe the desorption kinetics adequately.

The three-parameter TCFOKM was fitted to the desorption kinetic data and the model parameters are summarized in Table 6. Comparison of R^2 values (Tables 3 to 6) showed that the three-parameter TCFOKM fitted better than the two-parameter OSMTM, PFOKM and PSOKM to the desorption kinetic data. The result of TCFOKM analysis (Table 6) showed that the slow desorption fraction ($f_{2,d}'$) was much greater than the fast desorption fraction ($f_{1,d}$) for all PAHs. The size of $f_{1,d}$ decreased with aging time, which means an increase in the slow desorption fraction ($f_{2,d}'$) over aging time. The $f_{1,d}$ was in the order of naphthalene>phenanthrene>pyrene and thus, $f_{2,d}$ was in the order of pyrene>phenanthrene>naphthalene. This indicates that the more hydrophobic PAH has lower $f_{1,d}$ and higher $f_{2,d}$ than the less hydrophobic one. The first-order desorption rate constants in the fast ($k_{1,d}$) and slow ($k_{2,d}$) fractions were found to be 10^1-10^2 day^{-1} and 10^{-4}-10^{-3} day^{-1}, respectively. Opdyke and Loehr [28] discussed that the precision of $k_{2,d}$ is good only when many samples were taken near the time corresponding to $1/k_{2,d}$. This means that desorption kinetic data should be obtained over 1,000 days to have a reliable estimate of $k_{2,d}$. However, for desorption of PAHs from the sorbents used in this study, an extension of desorption time to 1,000 days is not practical, since fast desorption fraction reached desorption equilibrium within a few days. As a result, the precision of $k_{2,d}$ values obtained in this study may be unsatisfactory and only an order of magnitude estimate is useful, considering the timescale needed for the desorption in the slow desorption fraction. However, the precision of $k_{1,d}$ in this study would be useful since the time frame for the fast fraction is only 10^{-2} day ($=1/k_{1,d}$). The fast desorbing fraction of the sorbent is directly associated with the amount of organic contaminants available for immediate transport or biodegradation.

The four-parameter MTCFOKM was fitted to the desorption kinetic data, and the model parameters are summarized in Table 7. In terms of R^2 values, the four-parameter MTCFOKM was the best in fitting desorption kinetic data among the tested kinetic models due to the number of parameters involved. The slow desorption fraction ($f_{2,d}'$) was much greater than the fast desorption fraction ($f_{1,d}'$) for all PAHs. As aging time increased, fast desorption fraction ($f_{1,d}'$) decreased, while the slow desorption fraction ($f_{2,d}'$) increased. This indicates that aging played an important role in increasing the slow desorption fraction. The decrease in $f_{1,d}'$ means the increase in $f_{2,d}'$ as log K_{ow} increased, indicating that the more hydrophobic (or higher log K_{ow}) PAH had higher slow desorption fraction ($f_{2,d}'$) than the less hydrophobic one at all aging time frames. The first-order desorption rate constants in the fast ($k_{1,d}'$) and slow ($k_{2,d}'$) fractions were found to be 10^1-10^2 day^{-1} and 10^{-1}-10^0 day^{-1}, respectively.

Although both TCFOKM and MTCFOKM fitted well to the sorption and desorption kinetic data, MTCFOKM has advantages over

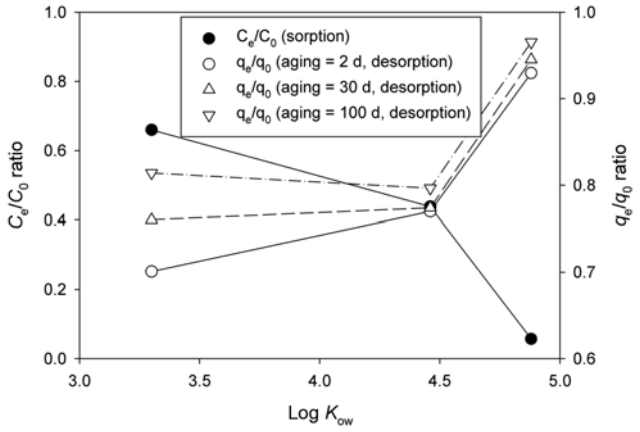

Fig. 3. Effect of hydrophobicty (log K_{ow}) on the C_e/C_0 ratio for sorption and the q_e/q_0 ratio for desorption.

TCFOKM. The equilibrium concentration in the soil phase, q_e, can be easily estimated by MTCFOKM (i.e., $q(t) \rightarrow q_e$ as $t \rightarrow \infty$ in Eq. (13)), but not by TCFOKM. The q_e may represent the remedial endpoint that can be estimated by desorption experiments. [29] Comparison of TCFOKM and MTCFOKM parameters shows that $k_{2,d}$ ($=10^{-4}$-10^{-3}) and $k'_{2,d}$ ($=10^{-1}$-10^{0}) are different in orders of magnitude. In this study, the precision of $k'_{2,d}$ was good only when many samples were taken near the time corresponding to $1/k'_{2,d}$ (=1 day). This means that desorption kinetic data of only for a few days is enough to have a reliable estimate of $k'_{2,d}$ in MTCFOKM, while over 1,000 days is need to estimate $k_{2,d}$ in TCFOKM. In this sense, MTCFOKM would be more realistic than TCKOFM since an extension of desorption time to only a few days would be enough to estimate q_e. The precision of $k_{1,d}$ of MTCFOKM would be also useful since the time frame for the fast fraction is only 10^{-2} day ($=1/k_{1,d}$). Moreover, in the desorption kinetics, Eq. (20), q(t) approaches the equilibrium sorbed amount (q_e) with time (i.e., $q(t) \rightarrow q_e$ as $t \rightarrow \infty$). This indicates that MTCFOKM can be used to estimate the remedial endpoint (i.e., q_e) without desorption experiment for a long time (>1 year).

In Fig. 3, the C_e/C_0 ratio for sorption decreased with hydrophobicity (log K_{ow}), but the q_e/q_0 ratio for desorption increased with log K_{ow} and aging time. It indicates that relatively larger fraction of PAH with higher hydrophobicity is more strongly sorbed onto the sediment and smaller fraction is desorbed. Therefore, PAH with high hydrophobicity is expected to reside in the desorption-resistant fraction in the aged coastal sediment [30]. However, further studies on the desorption kinetics and bioavailability using field-contaminated or aged sediments are needed to confirm the applicability of the newly derived MTCFOKM.

CONCLUSIONS

The sorption and desorption kinetics of naphthalene, phenanthrene and pyrene in coastal sediment were investigated. One-site mass transfer model (OSMTM), pseudo-first order model (PSOKM), pseudo-second-order model (PSOKM), two compartment first-order kinetic model (TCFOKM) and modified two compartment first-order kinetic model (MTCFOKM) were used.

OSMTM analysis indicates that apparent sorption and desorption equilibria were obtained within one day. At apparent equilibrium, the more hydrophobic (higher K_{ow}) PAH is sorbed more than the less one. The results of OSMTM analysis showed that the mass transfer coefficient (k_s) for sorption also decreased as the hydrophobicity increased. The apparent mass transfer coefficient for desorption (k'_d) increased over contact time except phenanthrene. However, both k_d and k'_d were not correlated to the K_{ow} values of the PAHs.

The sorption rate constant of PFOKM ($k_{p1,s}$) increased with the hydrophobicity of the PAHs. The desorption rate constant of PFOKM ($k_{p1,d}$) increased over contact time except phenanthrene. The sorption rate constant of PSOKM ($k_{p2,s}$) also increased as the log K_{ow} of the PAH increased. The more hydrophobic PAH had the higher $k_{p2,s}$. The desorption rate constant of PSOKM ($k_{p2,d}$) increased over contact time except phenanthrene. Comparison of PSOKM analysis for sorption and desorption kinetics (Table 5) showed that $k_{p2,d}$ was greater than $k_{p2,s}$ except phenanthrene at 100-d of contact time. However, both $k_{p2,d}$ and $v_{0,d}$ were not correlated with the hydrophobicity and aging time.

As expected, the three-parameter TCFOKM was better than the two-parameter OSMTM, PFOKM and PSOKM in describing sorption and desorption kinetics due to the presence of one more parameter in TCFOKM. In the sorption kinetics, the fast fraction ($f_{1,s}$) increased with the hydrophobicity of PAH, while the slow fraction ($f_{1,s}$) decreased. The first-order rate constants in the fast ($k_{1,s}$) and slow ($k_{2,s}$) sorption fractions were found to 10^{1}-10^{2} day^{-1} and 10^{-3}-10^{-2}, respectively. In the desorption kinetics, the slow desorption fraction ($f_{2,d}$) was much greater than the fast desorption fraction ($f_{1,d}$) for all PAHs. The size of $f_{1,d}$ decreased, while that of $f_{2,d}$ increased with aging time, indicating that slow desorption fraction ($f_{2,d}$) increases over contact time. The size of $f_{2,d}$ increased with log K_{ow}, while $k_{2,d}$ decreased indicating that the more hydrophobic PAH has higher slow desorption fraction ($f_{2,d}$) and slower desorption rate constant ($k_{2,d}$) than the less hydrophobic one. The first-order desorption rate constants in the fast fraction were much larger (10^{1}-10^{2} day^{-1}) than those in the slow fraction (10^{-4}-10^{-3} day^{-1}).

In terms of R^2 values, MTCFOKM was the best model in fitting both sorption and desorption kinetic data among the kinetic models tested due to the number of fitting parameters involved. As was in TCFOKM, the $f'_{1,s}$ increased with the hydrophobicity (log K_{ow}) of the PAH but the $f'_{1,d}$ decreased. The sorption rate constant of fast fraction ($k'_{1,s}$) was much greater than that of slow sorption fraction ($k'_{2,s}$). The fast sorption rate constant ($k'_{1,s}$) increased with log K_{ow} but the slow sorption rate constant did not. The desorption rate constants for fast fraction ($k'_{1,d}$) and for slow fraction ($k'_{2,s}$) were varied irregularly with aging time and hydrophobicity.

The results indicate that hydrophobicity (log K_{ow}) and aging are important factors in determining sorption and desorption kinetics of PAHs. The more hydrophobic PAH (i.e., higher log K_{ow}) is more likely to reside in slow desorption or desorption-resistant fraction in the coastal sediment over aging time and thus will have potential impacts on ecological risk. Therefore, further studies on the bioavailability of PAHs coupled to desorption kinetics are needed using field-contaminated or aged sediments. More focused mechanistic studies on the relationships between physicochemical properties of coastal sediments (e.g., organic carbon or black carbon content) and desorption kinetics are also needed. The results of this study can provide basic information on the risk assessment of PAHs in coastal

sediments.

ACKNOWLEDGEMENT

Financial support of this study was provided by Korea Science and Engineering Foundation, Grant # R05-2000-000-00355-0.

REFERENCES

1. J. Ibbotson and A. O. Ibhadon, *Mar. Pollut. Bull.*, **60**, 1136 (2010).
2. K. Grice, B. Nabbefeld and F. Maslen, *Organic Geochem.*, **38**, 1795 (2007).
3. G. P. Yang and X. Zheng, *Environ. Toxicol. Chem.*, **29**, 2169 (2010).
4. H. P. H. Arp, G. D. Breedveld and G. Cornelissen, *Environ. Sci. Technol.*, **43**, 5576 (2009).
5. W. P. Ball and P. V. Roberts, *Environ. Sci. Technol.*, **25**, 1223 (1991).
6. E. Eek, G. Cornelissen and G. D. Breedveld, *Environ. Sci. Technol.*, **44**, 6752 (2010).
7. W. Wu and H. Sun, *Chemosphere*, **81**, 961 (2010).
8. D. Kupryianchyk, M. I. Rakowska, J. T. C. Grotenhuis and A. A. Koelmans, *Environ. Pollut.*, **161**, 23 (2012).
9. X. Xia, J. Zhang, Y. Sha and J. Li, *J. Environ. Monit.*, **14**, 258 (2012).
10. J. Zhang and M. He, *J. Hazard. Mater.*, **184**, 432 (2010).
11. G. P. Yang, H. Y. Ding, X. Y. Cao and Q. Y. Ding, *Mar. Pollut. Bull.*, **62**, 2362 (2011).
12. W. Zheng, J. Lichwa and T. Yan, *Chemosphere*, **84**, 376 (2011).
13. A. T. Kan, G. Fu, M. A. Hunter and M. B. Tomson, *Environ. Sci. Technol.*, **31**, 2176 (1997).
14. A. A. Koelsmans, A. Poot, H. J. De Lange, I. Velzeboer, J. Harmsen and P. C. M. van Noort, *Environ. Sci. Technol.*, **44**, 3014 (2010).
15. D. Werner, H. K. Karapanagioti and D. A. Sabatini, *J. Contam. Hydro.*, **129-130**, 70 (2012).
16. L. Tremblay, S. D. Kohl, J. A. Rice and J. P. Gagne, *Mar. Chem.*, **96**, 21 (2005).
17. N. Ni and S. H. Yalkowsky, *Int. J. Pharm.*, **26**, 167 (2003).
18. J. McLachlan, *Can. J. Microbiol.*, **10**, 769 (1964).
19. J. C. Goldman and J. J. McCarthy, *Limnology Oceanogr.*, **23**, 695 (1978).
20. V. A. Nzengung, P. Nkedi-Kizza, R. E. Jessup and E. A. Voudrias, *Environ. Sci. Technol.*, **31**, 1470 (1997).
21. J. H. Kim, W. S. Shin, Y. H. Kim, S. J. Choi, W. K. Jo and D. I. Song, *Korean J. Chem. Eng.*, **22**, 857 (2005).
22. S. Oh, Q. Wu, D. I. Song and W. S. Shin, *J. Soil Groundwater Env.*, **16**, 79 (2011).
23. Y. Ho and G. McKay, *Water Res.*, **34**, 735 (2000).
24. R. A. Shawabkeh and M. F. Tutunji, *Appl. Clay Sci.*, **24**, 111 (2003).
25. S. Oh and W. S. Shin, *J. Environ. Sci. Health A*, **45**, 1150 (2010).
26. G. Cornellison, K. A. Hassell, P. C. M. van Noorst, R. Kraaij, P. J. van Erkeren, C. Dijkema, P. A. de Jager and H. A. J. Govers, *Environ. Pollut.*, **108**, 69 (1997).
27. G. Cornellison, H. Rigterink, B. A. Vrind, D. Th. E. M. ten Hulscher, M. M. A. Ferdinary and P. C. M. van Noorst, *Chemosphere*, **35**, 2405 (1997).
28. D. R. Opdyke and R. C. Loehr, *Environ. Sci. Technol.*, **33**, 1193 (1999).
29. G. Cornellison, P. C. M. van Noorst and H. A. J. Govers, *Environ. Sci. Technol.*, **32**, 3124 (1998).
30. A. T. Kan, W. Chen and M. B. Tomson, *Environ. Pollut.*, **108**, 81 (2000).